APPLIED AND ENVIRONMENTAL MICROBIOLOGY, May 2006, p. 3119–3129 Vol. 72, No. 5
0099-2240/06/$08.00+0 doi:10.1128/AEM.72.5.3119–3129.2006

Pyridine-2,6-Bis(Thiocarboxylic Acid) Produced by *Pseudomonas stutzeri* KC Reduces and Precipitates Selenium and Tellurium Oxyanions

Anna M. Zawadzka, Ronald L. Crawford, and Andrzej J. Paszczynski*

Environmental Biotechnology Institute, University of Idaho, Moscow, Idaho 83844-1052

Received 22 November 2005/Accepted 16 February 2006

The siderophore of *Pseudomonas stutzeri* KC, pyridine-2,6-bis(thiocarboxylic acid) (pdtc), is shown to detoxify selenium and tellurium oxyanions in bacterial cultures. A mechanism for pdtc's detoxification of tellurite and selenite is proposed. The mechanism is based upon determination using mass spectrometry and energy-dispersive X-ray spectrometry of the chemical structures of compounds formed during initial reactions of tellurite and selenite with pdtc. Selenite and tellurite are reduced by pdtc or its hydrolysis product H_2S, forming zero-valent pdtc selenides and pdtc tellurides that precipitate from solution. These insoluble compounds then hydrolyze, releasing nanometer-sized particles of elemental selenium or tellurium. Electron microscopy studies showed both extracellular precipitation and internal deposition of these metalloids by bacterial cells. The precipitates formed with synthetic pdtc were similar to those formed in pdtc-producing cultures of *P. stutzeri* KC. Culture filtrates of *P. stutzeri* KC containing pdtc were also active in removing selenite and precipitating elemental selenium and tellurium. The pdtc-producing wild-type strain KC conferred higher tolerance against selenite and tellurite toxicity than a pdtc-negative mutant strain, CTN1. These observations support the hypothesis that pdtc not only functions as a siderophore but also is involved in an initial line of defense against toxicity from various metals and metalloids.

Siderophores are iron-specific chelators that are produced and excreted by microorganisms under iron-limiting conditions as a part of an iron acquisition system. Some siderophores chelate metals other than iron, forming soluble or insoluble metal compounds and affecting the mobility and toxicity of those metals (8, 17, 47). Pyridine-2,6-bis(thiocarboxylic acid) (pdtc) is a siderophore produced by *Pseudomonas stutzeri* KC and *P. putida* DSM 3601 and DSM 3602 that has fortuitous carbon tetrachloride degradation activity (21, 30). Recent research has shown that pdtc promotes iron transport into the cell (25). *P. stutzeri* KC, its spontaneous pdtc-negative mutant CTN1, and other *P. stutzeri* strains also produce proferrioxamines (pFOs), which are probably their primary siderophores (A. Zawadzka et al., unpublished data). pdtc is a broad-range metal chelator; it chelates many transition metals, some heavy metals, lanthanides, and actinides. In general, micronutrient metals chelated by pdtc are soluble, while toxic metals form insoluble precipitates with pdtc (8, 39). Selenium and tellurium oxyanions are among the toxic metalloids precipitated by pdtc and pdtc-producing *Pseudomonas stutzeri* KC cultures.

In nature selenium is present in igneous rocks and fossil fuels (19). The element is a metalloid that can exist in four oxidation states. Under aerobic conditions, selenium is present as toxic and soluble selenate (SeO_4^{2-}) or selenite (SeO_3^{2-}) or as insoluble and nontoxic elemental selenium (Se^0). It is an essential micronutrient at low concentrations but is toxic at higher concentrations. Selenium is incorporated by organisms as selenide, and in high concentrations it substitutes for sulfur in cysteine and methionine, adversely affecting the integrity of proteins such as α-keratin and inhibiting the activity of enzymes such as glutathione peroxidase. Many bacteria have been shown to reduce selenite to Se^0, thereby eliminating its toxicity (27, 34, 31); however, the mechanism of detoxification is unclear. Elemental selenium deposits were found in the cytoplasm (18, 19), in the periplasmic space (14), and outside the cells (48) of various organisms, suggesting that different mechanisms might be involved. Selenium can be reduced enzymatically by broad substrate-specific nitrate reductases (35), molybdenum-containing enzymes (4), or specific selenate reductases in an energy-conserving process (36). It has been suggested that the cellular pool of thiols, including glutathione (GSH), is involved in the reduction and resulting detoxification of both selenite and tellurite (18, 43). When all reduced GSH in a cell is converted to GS-Se-SG, the cell loses its principal reducing buffer and thus its nonspecific defense against selenium toxicity. Finally, sulfate-reducing bacterial (SRB) biofilms were found to precipitate elemental selenium and sulfur during sulfate-reducing growth as a nonspecific means of selenium removal (16).

Tellurium is another highly toxic metalloid from group 16 of the periodic table. Tellurium is a relatively rare element found in nature in the form of metal tellurides (e.g., Pb, Cu, Ag, Au, and Sb). Industrial waste discharge sites can contain elevated concentrations of Te (2). Te(IV) as tellurite (TeO_3^{2-}) is more toxic to most gram-negative bacteria than Se(IV) in the form of selenite. The MIC for bacteria lacking resistance determinants is in the order of 1 to 2 μg ml^{-1} for TeO_3^{2-} (41) and 1 mg ml^{-1} for SeO_3^{2-} (44). This is the reason tellurite was used as an antibacterial agent for the treatment of bacterial infections in the preantibiotic era and is still a component of some selective growth media (41). Bacterial resistance to tellurite is poorly understood but is thought to be associated with tellurite reduction and precipitation of metallic tellurium (27, 34, 38). It

* Corresponding author. Mailing address: Environmental Biotechnology Institute, University of Idaho, Food Research Center 103, P.O. Box 441052, Moscow, ID 83844-1052. Phone: (208) 885-6318. Fax: (208) 885-5741. E-mail: andrzej@uidaho.edu.

has been suggested that tellurite entering cells can be reduced by membrane-associated nitrate reductases (1, 35). Once inside the cell, glutathione and other thiol-carrying molecules are the main mediators of tellurite reduction (43, 45). Also, terminal oxidases of the respiratory chain in gram-negative bacteria are involved in the reduction of tellurite (42). Other mechanisms, including cysteine-metabolizing enzymes and methyl transferases, may be important resistance mechanisms against tellurite toxicity (3, 41). Finally, similarly to what occurs with selenite, tellurite reduction and precipitation by sulfate-reducing bacteria has been reported (27).

Our current research investigated the nature of selenium and tellurium precipitates formed upon interaction with pdtc and the role of pdtc in detoxification of the bacterial environment. Here we propose a chemical mechanism for interactions of pdtc with selenite and tellurite. We identified the initial precipitates of Se and Te as insoluble selenides and tellurides of pdtc and the hydrolysis products of pdtc. Our data suggest that hydrolysis and oxidation of those initial precipitates leads to the formation of elemental Se and Te. We compared the reduction and precipitation products of selenite and tellurite mediated by synthetic, high-purity pdtc to the reaction products formed by pdtc-producing *P. stutzeri* KC and the pdtc-negative mutant strain CTN1. The nature of the precipitates formed in bacterial cultures of *P. stutzeri* KC was similar to the in vitro reaction products formed by synthetic pdtc. Electron microscopy analyses showed that in strain KC, elemental selenium and tellurium accumulated mainly extracellularly; however, pdtc did not completely prevent the accumulation of intracellular Se^0 and Te^0 under our experimental conditions. The use of pdtc by *P. stutzeri* KC to reduce selenite and tellurite is to our knowledge a unique system utilizing a siderophore to carry thiols to the extracellular environment that we describe here for the first time in bacteria. Our results add a novel function to the known activities of pdtc that is linked to detoxification of the bacterial habitat (5).

MATERIALS AND METHODS

Bacterial strains and culture conditions. The strains used in the present study included *P. stutzeri* strain KC (ATCC 55595, wild type, aquifer isolate; C. Criddle, Stanford University) (9) and strain CTN1 (spontaneous mutant of strain KC, University of Idaho culture collection) (21). The strains were maintained on tryptic soy agar plates (Difco, Detroit, Mich.). Media were prepared with deionized water purified to <18 mΩ resistivity using a WATER PRO PS filtration unit (Labconco, Kansas City, Mo.). Bacteria were grown in iron-limited acetate medium (DRM) at pH 7.8 (21) or iron-limited glucose-asparagine (GASN) medium at pH 7.0 (6) for 48 to 72 h at 30°C with constant shaking at 150 rpm.

MIC. The MICs of sodium selenite and potassium tellurite were determined on agar plates with DRM medium solidified with noble agar (Difco) prepared with increasing concentrations of Na_2SeO_3 or K_2TeO_3 (0.1 to 3 mM and 0.01 to 0.1 mM, respectively). The MIC was defined as the lowest concentration of inhibitor preventing growth of bacteria.

Interactions of pdtc with selenite and tellurite. pdtc was chemically synthesized using 2,6-pyridinedicarbonyl dichloride (Sigma, St. Louis, Mo.) as a starting compound (15). pdtc stock solutions in dimethylformamide (DMF) or acetonitrile were prepared fresh (100 mM). Stock solutions of Na_2SeO_3 (1 M) and K_2TeO_3 (100 mM) were prepared in deionized water. To monitor the formation of pdtc compounds with metalloids by using electrospray ionization-mass spectrometry (ESI-MS), the reaction mixtures of pdtc (1 and 2 mM) with selenite or tellurite (1 mM final concentrations of each) in DMF were prepared, filtered, and analyzed. For elemental analysis of the precipitates, reaction mixtures of pdtc with selenite or tellurite (10 mM final concentrations of each) in 0.2 M Tris-HCl buffer (pH 7.8) were prepared and incubated at 20°C for 7 days. The precipitates formed were collected by centrifugation (10,000 × *g* for 5 min), washed four times with water, resuspended in methanol, and analyzed by scanning electron microscopy and energy-dispersive X-ray spectrometry (SEM-EDS). To monitor the disappearance of selenite in the presence of *P. stutzeri* KC siderophores, reaction mixtures containing 0.5 mM selenite and 0.5, 1.0, 1.5, and 2.0 mM of (i) pdtc, (ii) proferrioxamine B mesylate salt (pFO B; Sigma, St. Louis, Mo.), or (iii) both pdtc and pFO B in 20 mM Tris-HCl buffer (pH 7.8) were incubated at 20°C for 72 h and filtered. The filtrates were analyzed for the presence of the remaining selenite by using high-performance ion chromatography (HPIC).

HPIC. Selenite remaining in the samples was monitored by using a DX-500 ion chromatography system (Dionex, Sunnyvale, Calif.) equipped with an ED40 electrochemical detector, IonPack AS16 column (Dionex), and IonPack ATC-1 ion suppressor (Dionex). The mobile phase consisted of 100 mM NaOH and water (solvents A and B, respectively). For selenite remaining in reaction mixtures with pdtc or pFO B, elution was performed by using a linear gradient of 5 to 10% A over 10 min and 10 to 100% over 20 min, followed by 100% A for the next 10 min at a flow rate of 1 ml min^{-1}. The concentration of selenite remaining in the reaction mixture was compared to the concentration of selenite in the control samples without added siderophores. For selenite remaining in the bacterial cultures and culture filtrates, elution was performed with a linear gradient of 5 to 20% A over 10 min and 20 to 30% over 20 min, followed by 100% A for the next 10 min at a flow rate of 1 ml min^{-1}. The concentration of selenite remaining was calculated relative to the concentration of the selenite in the sterile-medium controls.

Microbially mediated selenium and tellurium precipitation. Bacteria (strains KC and CTN1) were grown in DRM or GASN medium to the late logarithmic phase. To the cultures, 0.5 mM selenite or 0.05 mM tellurite was added, and the flasks were incubated for another 24 h until cultures turned orange-red or black, respectively. The cells were harvested for electron microscopy analysis. Another batch of cultures was allowed to stand at room temperature for several days, the cells were lysed with lysozyme (2 mg ml^{-1}), and the metalloid precipitates were centrifuged and washed several times with water to remove the remaining media and cell components. The precipitates were analyzed by using SEM-EDS. To monitor the activity of bacterial cell-free spent cultures in selenium and tellurium precipitate formation, 48-h cultures of *P. stutzeri* KC and CTN1 in GASN medium were centrifuged (10,000 × *g* for 20 min) and filtered through 0.22-μm-pore-size syringe filters. The pdtc concentration in strain KC spent medium was assayed spectrophotometrically (24). Selenite (0.1 mM) and tellurite (0.05 mM) were added, and the samples were incubated at room temperature for 7 days. Selenium and tellurium precipitates formed only in strain KC. Precipitates were washed extensively with water and subjected to SEM-EDS analysis.

Removal of selenite by bacterial cultures. To monitor the removal of selenite by bacterial cultures and spent medium components, *P. stutzeri* KC and CTN1 were grown in GASN medium for 48 h. Half of a culture was used as a cell-containing 48-h culture, while the remainder was centrifuged (10,000 × *g* for 20 min) and filtered through 0.22-μm-pore-size syringe filters to obtain cell-free spent media. Selenite (0.1 mM) was added to the cultures and culture filtrates, and the samples were incubated for 24 h at 30°C with constant shaking at 150 rpm. Selenite remaining in the media was measured by using HPIC. The pdtc concentration in strain KC spent medium was assayed spectrophotometrically (24).

ESI-MS/MS. The reaction mixtures containing pdtc and tellurite or selenite were analyzed by using electrospray ionization-tandem mass spectrometry (ESI-MS/MS; Quattro II; Waters-Micromass, Ltd., United Kingdom). Samples were delivered into the source at a flow rate of 5 μl min^{-1} with a syringe pump (Harvard Apparatus, South Natick, Mass.). A potential of 2.8 kV was applied to the electrospray needle, and the sample cone voltage was maintained at 15 V. Detector resolution was set at 15,000, and the source temperature was kept constant at 100°C. For structural analysis, daughter fragmentation (MS/MS) was performed. The collision cell was operated at 10 to 15 eV with argon gas pressure adjusted to give ca. 80 to 90% parent ion fragmentation. All MS and MS/MS spectra were an average of 18 scans over a mass range of 20 to 1,000 Da.

SEM-EDS. Bacterial cells grown in the presence of selenite and tellurite were collected and processed for SEM-EDS analysis. The cells were fixed with 2% (wt/vol) glutaraldehyde in 0.2 M cacodylate buffer, dehydrated with ethanol of increasing concentrations (40, 50, 70, 80, 90, 95, and 100%), dried on polycarbonate membranes (Millipore, Bedford, Mass.) in a critical point drier, and carbon coated. Precipitates formed by pdtc and bacterial cultures were resuspended in methanol and mounted on carbon tape. Specimens were examined with a LEO Supra 35 VP FESEM equipped with a Thermo Electron System Six EDS (Zeiss, Thornwood, N.Y.). Accelerating voltages used are shown in the microscopy image figures. Element ratios were calculated as averages of three to five sample measurements.

TABLE 1. Summary of ESI-MS spectra of peaks corresponding to charged tellurides of pdtc and the pdtc hydrolysis product pctc[a]

m/z			Charge	Molecular composition
^{130}Te	^{128}Te	^{126}Te		
326.8	324.8	322.8	−1	(pdtc)Te
524.7	522.7	520.7	−1	$(pdtc)_2$Te
261.9	260.9	259.9	−2	$(pdtc)_2$Te
508.7	506.7	504.7	−1	(pdtc)(pctc)Te
721.6	719.6	717.6	−1	$(pdtc)_3$Te
360.4	359.4	358.4	−2	$(pdtc)_3$Te
705.6	703.6	701.6	−1	$(pdtc)_2$(pctc)Te

[a] *m/z* values are given for the three most abundant tellurium isotopes of the following natural abundance: ^{130}Te 34.40%, ^{128}Te 31.79%, and ^{126}Te 18.71%. Te-containing compounds were recognized based on this characteristic Te isotope distribution pattern.

Transmission electron microscopy (TEM) and EDS. Bacterial cells grown in GASN medium in the presence of selenite and tellurite were harvested, fixed with 2% (wt/vol) glutaraldehyde in 0.1 M cacodylate buffer or 2% paraformaldehyde–1.25% glutaraldehyde in 0.1 M phosphate buffer, dehydrated with ethanol and acetone, and embedded in Spurr Low Viscosity epoxy resin (Polysciences, Warrington, Pa.). Sections were not stained to avoid any interference during EDS analysis. Samples were analyzed with a JEOL model JEM 1200 EX electron microscope (JEOL, Tokyo, Japan) operating at 100 kV. The EDS spectra were recorded with a KEVEX Micro-X 7000 analytical spectrometer (Kevex Co., Foster City, Calif.).

RESULTS

MICs of selenite and tellurite. The MICs of sodium selenite determined for pdtc-producing strain KC and pdtc-negative mutant CTN1 in iron-limited medium were 3 and 0.5 mM, respectively. The MICs of potassium tellurite determined for strains KC and CTN1 were 0.1 and 0.075 mM, respectively.

Interactions of pdtc with selenite and tellurite. Upon pdtc mixture with aqueous selenite solution, a white-yellowish precipitate formed, which subsequently changed to an orange-red color, indicating formation of amorphous elemental selenium. Similarly, when pdtc was mixed with a tellurite solution, an orange precipitate formed which gradually changed to black, the color of elemental tellurium. Both initially formed precipitates were soluble in DMF; therefore, the DMF solution was used for ESI-MS/MS analyses. Tellurium-containing compounds were identified as a series of peaks in ESI-MS spectra with a pattern of *m/z* and intensity corresponding to the characteristic isotope distribution of tellurium (Table 1). Several types of differently charged pyridine-2,6-bis(thiocarboxyl) tellurides were identified: $[pdtcTe]^{-1}$, $[(pdtc)_2Te]^{-1}$, $[(pdtc)_2Te]^{-2}$, $[(pdtc)_3Te]^{-1}$, and $[(pdtc)_3Te]^{-2}$. Tellurides containing two or three pdtc and pctc (the pdtc hydrolysis product, pyridine-2-carboxylic-6-thiocarboxylic acid) molecules were observed (Table 1). The presence of Te-containing compounds with different pdtc-to-Te ratios depended on the molar ratios of pdtc to tellurite used for the reactions. When equimolar concentrations were used, (pdtc)Te was detected mainly with some $(pdtc)_2$Te. When a twofold-higher pdtc concentration was used for the reaction, $(pdtc)_2$Te was predominant, with some $(pdtc)_3$Te detectable. In addition, peaks corresponding to the polymerized pdtc and pctc molecules were detected: $[(pdtc)_2]^{-1}$, *m/z* 394.9; $[(pdtc)_3]^{-2}$, *m/z* 295.4; $[(pdtc)(pctc)]^{-1}$, *m/z* 378.9; and $[(pdtc)(pctc)_2]^{-2}$, *m/z* 279.4. In most samples, peaks corresponding to the pdtc hydrolysis products dipicolinic acid [pyridine-2,6-bis(carboxylic acid)] (dpa) ($[dpa]^{-1}$, *m/z* 166.1) and pyridine-2-thiocarboxylic acid (ptc) ($[ptc]^{-1}$, *m/z* 138.0) were found (spectra not shown). Structures of the pdtc tellurides were proposed based on the fragmentation patterns of the parent molecules seen during ESI-MS/MS daughter analysis (Fig. 1). The reaction mixture of pdtc with selenite was also analyzed. The pdtc selenides were not detectable by ESI-MS. However, the initial color change indicated the formation of pdtc selenide compounds analogous to that identified for tellurium. Only polymerized pdtc and pctc molecule peaks were detected in pdtc-treated selenite solutions.

The concentration of selenite remaining after reaction with chemically synthesized pdtc at pH 7.8 was also determined (Table 2). The complete removal of selenite was observed when a 4:1 pdtc/selenite molar ratio was present in solution. The decrease in selenite concentration was accompanied by a change in precipitate color to orange-red. A synergistic effect was observed when chemically pure proferrioxamine B was present together with pdtc where selenite was completely removed in the presence of a 2:1 molar ratio of both siderophores compared to selenite. In the reaction where pFO B alone was present, a maximum of ca. 40% of the selenite was

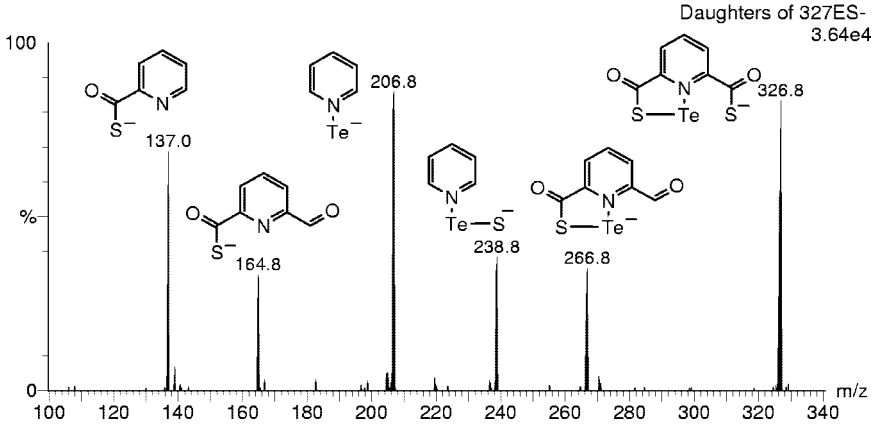

FIG. 1. ESI-MS/MS spectrum showing fragmentation of pdtc telluride $[(pdtc)^{130}Te]^{-1}$ (*m/z* 327). The structures of daughter fragments are shown next to the fragment anion peaks.

TABLE 2. The percentage of selenite remaining after incubation with chemically synthesized siderophores of *P. stutzeri* KC, pdtc, and pFO B[a]

Siderophore concn (mM)	% SeO_3^{2-} remaining		
	pdtc	pFO B	pdtc + pFO B
0.5	88.1 (0.7)	96.6 (0.7)	57.7 (0.3)
1.0	56.9 (9.2)	67.5 (0.6)	0.2 (0.3)
1.5	16.2 (4.4)	60.0 (0.9)	ND
2.0	0.4 (0.03)	63.4 (0.04)	ND

[a] The selenite remaining of 0.5 mM added was measured using HPIC and values are the means of triplicate measurements, with standard deviations given in parentheses. ND, not detected.

removed, and no orange color indicative of elemental selenium appeared.

The appearance and composition of precipitates formed abiotically upon mixing pdtc solution with selenite and tellurite were examined by using SEM-EDS (Fig. 2B and F and 3B). As observed by SEM, the selenium particles were spherical, ranging from 300 to 1,000 nm in diameter, whereas the tellurium precipitate appeared mostly amorphous, with some structured particles of <10 nm in diameter. In both cases, selenium or tellurium was detected and accompanied by sulfur. On average, the selenium precipitate contained sulfur in a ratio of 1:2.09 (Se:S), whereas the tellurium precipitate was composed

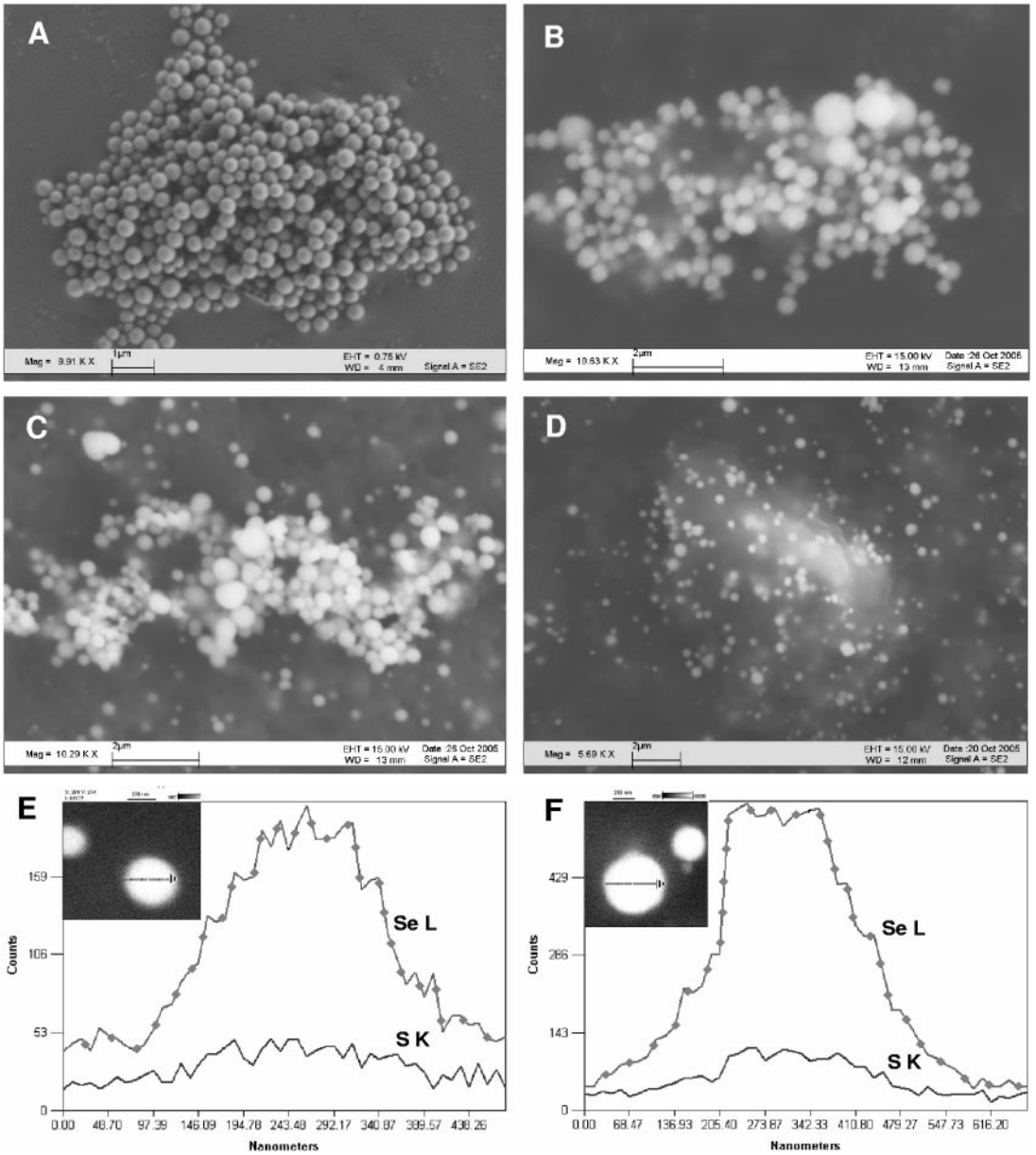

FIG. 2. SEM images of selenium precipitates formed: in *P. stutzeri* KC culture filtrate containing nearly 0.1 mM pdtc produced by bacteria (A), abiotically by chemically synthesized pdtc (B), in *P. stutzeri* KC culture (C), and in bacterial cultures of *P. stutzeri* CTN1 (D). (E and F) EDS line scans of selenium spheres formed in *P. stutzeri* KC culture filtrate (E) and abiotically by chemically synthesized pdtc (F). Accelerating voltage, 15.0 kV.

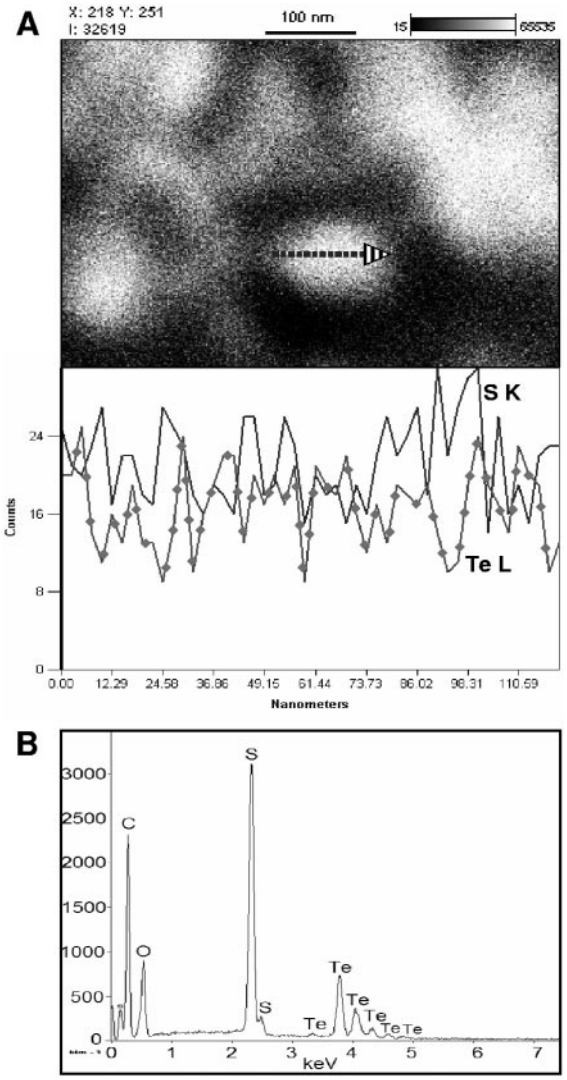

FIG. 3. (A) SEM image and EDS line scan across tellurium precipitate formed in *P. stutzeri* KC culture filtrate; (B) EDS spectrum of tellurium precipitate formed by pdtc.

of Te and S in a ratio of 1:4.05, calculated from the atom percentage present. When the precipitates were subjected to extensive washing, the content of sulfur decreased by about 10-fold to, for example, an Se/S ratio of 1:0.2 (Fig. 2F).

We also observed that pdtc reacted in a similar manner with Te(VI) (tellurate) but at a much lower rate, on the order of days instead of minutes compared to Te(IV). Although the reactions proceeded more slowly, the same reaction products were observed (data not shown).

Removal of selenite by bacterial cultures. Bacterial cultures of strain KC and CTN1 and spent culture filtrates were examined for their abilities to reduce selenite. The remaining percentage of selenite was calculated as a mean of triplicate determinations and relative to the selenite concentration in uninoculated culture media. Cultures of both strains were effective in the complete removal of 0.1 mM selenite added at 24 h of growth; no remaining selenite was detected by using HPIC. The culture filtrate (48 h) of strain KC contained 92 μM pdtc and reduced 69.3% of the selenite added. The culture filtrate of strain CTN1 was able to reduce 43.5% of the selenite despite the lack of pdtc. However, the red precipitate of Se^0 appeared only in the strain KC culture filtrate.

Selenium and tellurium precipitates formed in bacterial cultures. The precipitates formed in bacterial cultures of strain KC and CTN1 and culture filtrates of strain KC after the addition of selenite and tellurite were examined by using SEM-EDS (Fig. 2A and C to E and 3A). The EDS spectra showed characteristic selenium emission lines at 1.37 keV (SeLα), 11.22 keV (SeKα), and 12.49 keV (SeKβ); tellurium gave the expected emission lines at 3.77, 4.03, 4.3, and 4.57 keV, corresponding to the $TeL\alpha_1$, $TeL\beta_1$, $TeL\beta_2$, and $TeL\gamma_1$ transitions, respectively. Only the cell-free culture filtrate of strain KC containing about 95 μM pdtc was active in selenite and tellurite reduction and element precipitation. Precipitates were identified as containing elemental Se and Te based on SEM-EDS analysis and characteristic physical properties of Se and Te in amorphous elemental form. Particles of selenium were spherical and contained Se and S in a ratio ranging from 1:0.13 to 1:1.16 (Se:S) depending on the extent of the precipitate washings applied (Fig. 2A and E). The tellurium precipitate was composed of very fine particles that were not resolved using SEM. EDS line scans across Te particle aggregates showed that these particles are a few nanometers in size (Fig. 3A). EDS point analysis revealed that sulfur distribution within the Te precipitate was uneven, ranging from 1:0.12 to 1:3 (Te:S) (data not shown). In precipitates formed in bacterial cultures, selenium and tellurium were detected, together with several other elements that are components of culture media and cell debris. In strain KC, selenium was accompanied by sulfur in a ratio of 1:1.49. The ratio was only 1:0.34 for strain CTN1. The selenium particles formed by strain KC were spherical and averaged 100 to 700 nm in diameter (Fig. 2C). The selenium precipitate formed by strain CTN1 was often associated with cell debris and contained particles ranging in size from several nm to 650 nm in diameter (Fig. 2D). It was not possible to disperse the tellurium precipitate formed in bacterial cultures into individual particles where the precipitate was observed as aggregates of one to several micrometers in size. The tellurium precipitate was associated with strain CTN1 cellular debris in particular. The sulfur content was higher in the precipitate formed in strain KC cultures (1:3.4 [Te:S]) than in CTN1 cultures (1:0.2 [Te:S]), where the EDS sulfur signal was similar to the background S signal (images and EDS spectra not shown).

Location of selenium and tellurium precipitates in bacterial cultures. To identify whether selenium and tellurium precipitates formed outside the bacterial cells, the cells of strains KC and CTN1 from the cultures that reduced the metalloid were harvested, gently washed, and fixed to allow for examination by using SEM-EDS. It was observed that in strain KC, large amounts of selenium precipitate were visible as spherical aggregates outside the bacterial cells (Fig. 4A). Identification of the selenium within the precipitate was confirmed by EDS analysis. In strain CTN1, very few extracellular selenium particles were present (Fig. 4B), and EDS elemental maps showed a selenium signal in association with the cells (data not shown). The tellurium precipitate and EDS tellurium signal in whole-cell mounts of both strains was associated with cell mass, and

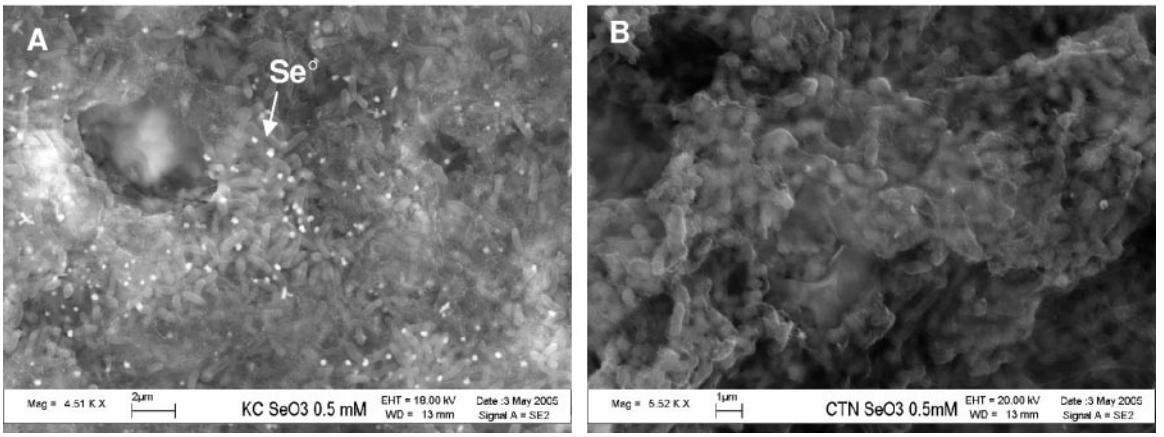

FIG. 4. Scanning electron micrographs of whole mounts of cells of *P. stutzeri* KC (A) and CTN1 (B). Both strains were grown in iron-limited medium supplemented with 0.5 mM sodium selenite. Selenium granules are visible as extracellular deposits indicated by an arrow.

no distinguishable extracellular particles were observed (data not shown). To examine the intracellular localization of the precipitates, bacterial cells were prepared for TEM observations. TEM images of cross-sections of the bacteria that reduced selenium revealed high-electron-density spherical selenium particles inside the cells (Fig. 5A and B). Particle elemental composition was confirmed by EDS analysis, and only selenium lines were detected and were not accompanied by sulfur (Fig. 5E). KC cells had fewer selenium particles inside than CTN1 cells, but the intracellular selenium content was not quantified. TEM images of bacteria grown in the presence of tellurite also revealed the presence of elemental tellurium deposits inside the cells (Fig. 5C1 and C2 and D1 and D2). Te^0 deposits were clearly associated with cell membranes. Strain CTN1 cells appeared to have slightly more tellurium deposited inside the cells than strain KC cells tested under similar conditions. Similarly to what we observed with selenium intracellular deposits, EDS spectra showed that tellurium was not accompanied by sulfur deposition (Fig. 5F).

DISCUSSION

pdtc was found to form poorly soluble precipitates when mixed with selenite or tellurite, and these precipitates were subsequently converted to elemental selenium and tellurium. To our knowledge, this is the first observation of a siderophore-type molecule being involved in reduction and precipitation of metalloid oxyanions. Our observations also add a novel function (metalloid detoxification) to the various previously described pdtc activities (8, 21, 25, 37, 39). Based on our analyses, we propose a mechanism for pdtc chemical interactions with tellurium (Fig. 6). Initially, pdtc hydrolysis and oxidation leads to Te(IV) reduction, and the remaining pdtc and pdtc hydrolysis products form orange-colored pdtc tellurides. The hydrolysis of pdtc also leads to the release of H_2S (8, 26), and Te(IV) is abiotically reduced by H_2S via a mechanism similar to that described for SRB (16). pdtc then binds Te through its carbonyl sulfide moieties, forming intramolecular tellurotrisulfide or intermolecular tellurotrisulfides analogous to selenodiglutathione (18). The pdtc tellurides bear no charge and therefore are poorly soluble in water. Finally, hydrolysis of pdtc tellurides leads to the formation of black elemental tellurium accompanied by coprecipitation of sulfur that originates from pdtc's carbonyl sulfide groups. The color of the initial precipitate formed differs from that of elemental tellurium. Thus, observations of physical appearance and the confirmed presence of pdtc tellurides support our proposed mechanism of interaction of pdtc with telluride. The same or a similar mechanism is possible for selenium interactions with pdtc. However, we were unable to identify pdtc selenides by using ESI-MS, probably due to their lower solubility, lower ionization efficiency, or instability in the ESI-MS source compared to pdtc tellurides. The initial whitish color of the selenite-derived precipitate, which again is different from the orange-red color of elemental Se, and the presence of oxidized pdtc polymers in the reaction mixture detected by ESI-MS suggest a similar type of interaction. One can also expect selenium to have chemistry similar to that of tellurium since both elements belong to group 16 of the periodic table. Pdtc-mediated reactions would be analogous to selenium interactions with GSH in the Painter reaction (32). GSH reacts with selenite to form selenodiglutathione (GS-Se-SG), which is a substrate for glutathione reductase. Selenodiglutathione reduction results in formation of unstable glutathione selenopersulfide ($GS\text{-}Se^-$) that dismutates into elemental selenium and reduced GS^- (13). Since tellurite is also thiol reactive, it is also expected to follow a Painter-type reaction (43, 45).

The nature of the compounds pdtc forms with the metalloids tellurium and selenium must be different from the complexes the siderophore forms with metals. pdtc forms coordination compounds (complexes) with many metals, but Se and Te behave essentially as nonmetals, with increasing metallic character from Se to Te. Also, Se and Te are more electronegative than metals, with electronegativities similar to sulfur; therefore, the character of the bonds they can form with sulfur is more covalent than ionic (22). Consequently in the compounds that pdtc can form with Se and Te, the sulfur atoms of pdtc are expected to covalently bind the metalloids, thus forming pdtc selenides and tellurides. The structure of pdtc tellurides was elucidated by using ESI-MS/MS only when they were solubilized in DMF (Fig. 1). Presumably, the solubility of investi-

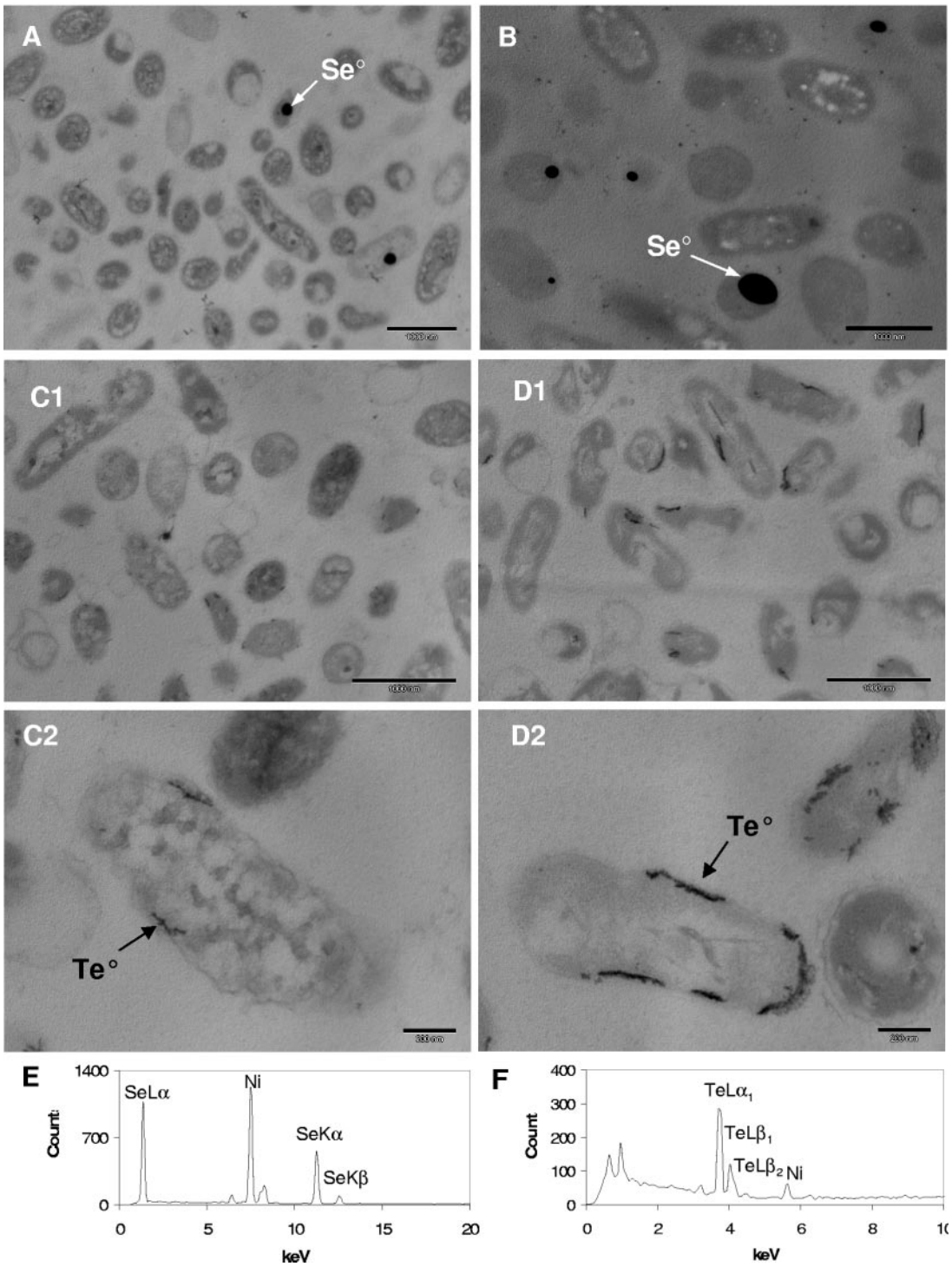

FIG. 5. TEM images of bacteria grown in the presence of selenite and tellurite. (A) *P. stutzeri* KC at 0.5 mM selenite; (B) *P. stutzeri* CTN1 at 0.5 mM selenite; (C1 and C2) *P. stutzeri* KC at 0.05 mM tellurite; (D1 and D2) *P. stutzeri* CTN1 at 0.05 mM tellurite. Arrows indicate Se^0 and Te^0 deposits localized in the electron-dense particles inside the cells. The compositions of the deposits were confirmed by EDS analysis. (E) Spectrum of intracellular Se^0 deposit; (F) spectrum of intracellular Te^0 deposit. The Ni signal is due to the grid used for microscopy.

gated compounds in water was too low for MS detection. The fragmentation of the $[(pdtc)Te]^{-1}$ molecular ion also indicated a strong interaction between pdtc's pyridine nitrogen and tellurium atoms that led to the pyridine-Te fragment ion observed (Fig. 1).

The appearance and composition of the metalloid precipitates formed abiotically by chemically synthesized pdtc were compared to those of the precipitates formed by bacterial cultures of *P. stutzeri* KC and CTN1 and by culture filtrates of strain KC (Fig. 2 and 3). Only in the cell-free spent culture

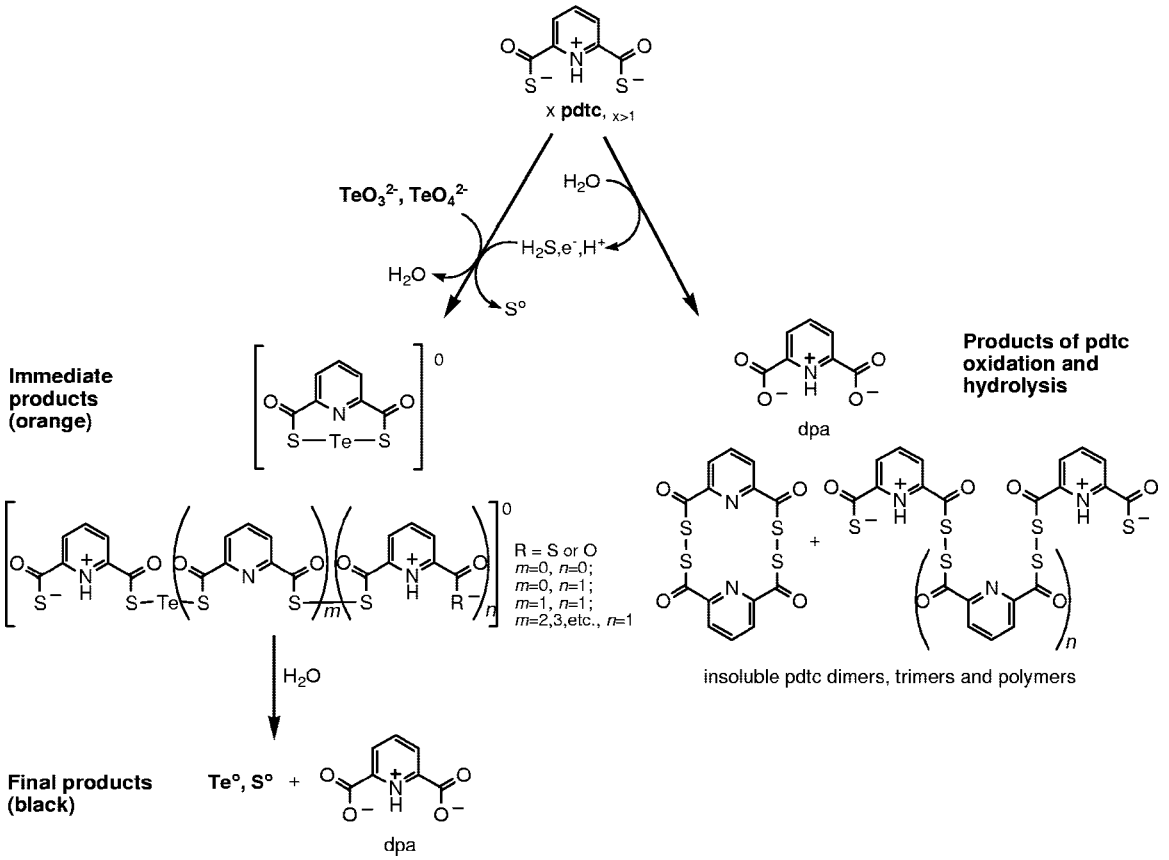

FIG. 6. Proposed interactions of pdtc with tellurium. Tellurite and tellurate are reduced by pdtc or its hydrolysis product H_2S and subsequently bound by pdtc and pdtc hydrolysis products, including pctc and dpa. Initially formed zero-valent tellurides release elemental Te and Se. The reaction pathways are shown qualitatively, not stoichiometrically. Using ESI-MS, all products were detected as charged molecules, and their structures were deduced from ESI-MS/MS daughter analysis (see Table 1 and Fig. 1).

filtrate of *P. stutzeri* KC containing pdtc did the addition of selenite result in a red precipitate. When tellurite was added to the cell-free spent culture filtrate of *P. stutzeri* KC, the filtrate changed color to dark brown, suggesting pdtc as a reducing agent. The appearance and elemental makeup of these precipitates were more similar to those of precipitates formed in an abiotic reaction with pdtc than in the bacterial cultures of strain CTN1. In the precipitates formed in strain KC cell-free culture filtrates and cultures containing bacteria, the presence of elevated amounts of sulfur was similar to that seen in the precipitates formed by chemically synthesized pdtc. These observations suggest that pdtc is mainly responsible for extracellular reduction and precipitation of these metalloids. The lower content of sulfur in biologically formed precipitates of strain KC than in those formed during pure pdtc-mediated reactions can be explained by the fact that the precipitate purified from the bacterial cultures contained both extracellular particles formed by pdtc and intracellular deposits that did not contain sulfur (Fig. 5E and F). pdtc reactivity toward selenite results in a precipitate with properties similar to those of extracellular selenium precipitated by SRB (16). The SRB-produced precipitate contained both elemental selenium and sulfur in a ratio of 1:1.5 as opposed to 1:2 predicted by the reaction equation $SeO_3^{2-} + 2HS^- + 4H^+ \rightarrow Se^0 + 2S^0 + 3H_2O$. The presence of sulfur in selenium and tellurium precipitates formed by pdtc is indicative of pdtc thiol group involvement in metalloid oxyanion reduction, and elemental selenium and tellurium precipitation was a result of pdtc and pdtc selenide and telluride hydrolysis. The reduction of SeO_3^{2-} to Se^0 requires four electrons and six protons; therefore, 2 moles of pdtc (four thiol equivalents) would be required to reduce 1 mol of selenite (or tellurite). Our results showed, however, that only a fourfold-higher molar concentration of pdtc completely removed selenite (a twofold excess over theoretical) and only a twofold higher concentration in the presence of pFO B (Table 2). We speculate that pFO B catalytically assisted with electron transfer in the reduction reaction when complexed with traces of transition metals. Similarly, the disappearance of ~40% of the selenite from CTN1 culture filtrates may be attributed to unidentified interactions of selenite with proferrioxamines produced by this strain (data not shown), which is similar to what was found for chemically pure pFO B (Table 2), where no elemental selenium formation was observed. The higher sulfur content of the tellurium precipitate formed by pdtc (1:4 ratio of Te to S) may indicate that the precipitate contains some pdtc molecules as pdtc tellurides (Table 1) or polymerized pdtc. The abundance of tellurides with different pdtc/Te ratios depended on the initial molar ratio of pdtc to tellurite used in the reactions and was consistent with the known dependence of such reaction products on

the ratios of the reactants in the transformation of selenite by GSH (18). In contrast, EDS analysis of intracellular selenium and tellurium precipitate did not show the presence of significant amounts of sulfur (Fig. 5E and F). Similarly, both washed selenium and tellurium precipitates formed by strain CTN1 had low or no sulfur content. This indicates that the mechanisms involved in intracellular Se and Te deposit formation are different from those occurring extracellularly.

Based on the elemental composition and spherical shape of selenium particles compared to the amorphous character of tellurium precipitates formed by pdtc, it appears that the particle relates directly to the properties of the elements involved. Elemental selenium is known to have six allotropic forms; the red nonmetallic forms have three types of eight-member rings (Se_8) packed differently in the crystals and one amorphous form containing polymeric Se chains (23). Oremland et al. (31) proposed that selenium nanospheres produced by Se-respiring bacteria are composed of interconnected three-dimensional nets of selenium where both ring (Se_8) and chain structures exist and should result in a spherical shape. Se spheres formed by reaction with pdtc may have a similar structure where sulfur, which can also form polymeric ring structures, seems to be intercalated in the Se matrix. This suggestion follows from the observation that the sulfur content in Se particles formed by pdtc was variable and depended on the conditions during which the particles formed. Also, extensive washing of selenium precipitates resulted in a lower S content as observed in our SEM-EDS studies. On the other hand, tellurium has only one crystalline form that is similar to gray Se and contains infinite spiral chains of Te atoms with metallic interactions stronger than in Se (23), a characteristic that may explain the unstructured character of Te precipitates formed by pdtc.

Electron microscopy and EDS analyses also allowed for localizing the sites of elemental selenium and tellurium deposition in bacterial cultures. SEM images of strain KC cultures clearly showed the abundance of extracellular spherical deposits of selenium (Fig. 4A) similar to those found in SRB biofilms (16). SEM images of strain CTN1 whole-cell mounts revealed little extracellular selenium precipitate (Fig. 4B). It is possible that sample preparation for SEM removed part of the extracellular precipitates, but since the treatment was the same for samples of both strains, we conclude that any losses were proportional to the original abundance. Therefore, we can still compare the quantities of extracellular precipitates found in strain KC and CTN1 cultures. TEM analysis showed the presence of spherical electron-dense selenium particles present inside the cells of both strains KC and CTN1 (Fig. 5A and B); however, intracellular selenium deposits were observed to be more abundant in strain CTN1. Clearly, pdtc was able to reduce and precipitate large amounts of selenium outside strain KC cells but, in the culture conditions used here, did not completely prevent the entrance of selenite into the cells. We do believe that extracellular precipitation plays a significant role in preventing selenite toxicity, as was shown by our examinations of MICs for selenite in stationary cultures of strain KC. Tellurium precipitates were more difficult to observe via SEM, and no clearly visible precipitates were located extracellularly. SEM-EDS analysis indicated the presence of tellurium in association either with cells or extracellular matter, but no distinctive particles were seen in whole-cell mounts, possibly due to their fine particulate structure (images not shown). TEM images revealed the presence of intracellular Te^0 deposits associated with cell membranes of both strains (Fig. 5C and D). Although strain KC cells had less tellurium deposited intracellularly, pdtc production did not prevent the entrance of tellurite into cells under our experimental conditions. In addition, the tellurite MIC for strain KC was not considerably higher, as was the case for selenite, demonstrating a higher toxic effect of tellurite and less effective pdtc-mediated detoxification. In addition, tellurite was shown to be ~1,000-fold more toxic to *Escherichia coli* than selenite (43); however, pdtc was previously shown to protect four other bacterial strains that do not produce pdtc from Te toxicity (8). This suggests a decreased bioavailability of tellurium caused by pdtc.

In other studies, selenium and tellurium precipitates were found in different cellular locations or extracellularly depending on the mechanism of their formation, and detoxification mechanisms were suggested to be different between selenite and tellurite (16, 19, 20, 28, 31, 42). To refine the findings of tellurium precipitate localization, the biofilms of strain KC and CTN1 were grown in the presence of tellurite and analyzed by SEM-EDS after only gentle washing (data not shown). No pronounced differences were found, and we concluded that the extremely fine size of the tellurium precipitate did not allow for its visualization in extracellular locations by using SEM.

pdtc-mediated selenium and tellurium precipitation is not the only defense mechanism against metalloid toxicity that *P. stutzeri* KC possess. In strain CTN1, a pdtc-negative mutant of strain KC, the mechanism of Se and Te reduction has to be associated exclusively with intracellular mechanisms since no selenium or tellurium precipitation occurred in the cell-free spent culture filtrate of CTN1, but cell-containing cultures were active in metalloid reduction. We can view those intracellular mechanisms as a second line of defense in strain KC. Selenite and tellurite that circumvent the initial line of *P. stutzeri* KC protection (extracellular pool of pdtc) can enter cells through sulfate (selenite) and phosphate (tellurite) uptake systems (41). Once in the periplasmic space or cytoplasmic membrane vicinity, selenite and tellurite can be acted on by the terminal oxidases of the respiratory chain (42) or nitrate reductases, as shown for other denitrifying bacteria (1, 35). Since in our experiments bacteria were grown aerobically, the latter mechanism is unlikely, although Sullivan et al. (40) reported the presence of constitutively expressed nitrate reductase in another strain, *P. stutzeri* ATCC 14405, and such an enzyme might be expressed by KC as well. Finally, selenite and tellurite can enter the cytoplasm, where they can be reduced by glutathione and/or other reductants (18, 43, 45). The location of intracellular metalloid deposits in *P. stutzeri* KC and CTN1 indicates the involvement of a membrane-associated mechanism in the case of tellurite reduction and a cytoplasm-located selenite reduction system. This observation is in line with the recent findings of Lohmeier-Vogel et al. (28), who suggested different routes for selenite and tellurite reduction within *E. coli* cells.

We can conclude that in addition to all other previously known pdtc functions, pdtc production and excretion serves as an extracellular metalloid reduction and thus an environmental detoxification mechanism for *P. stutzeri* KC. The conclusion that pdtc mediates toxic selenite reduction and Se^0 precipita-

tion was confirmed by selenite removal in abiotic reactions (Table 1), as well as by spent culture filtrate of the pdtc-producing strain KC. The compositions and appearances of selenium and tellurium precipitates formed in *P. stutzeri* KC cultures and in abiotic reaction of pure pdtc were similar, indicating a common route for their formation. pdtc can be considered a preventive measure against selenite and tellurite toxicity before these metalloid oxyanions enter bacterial cells. Thiol-containing molecules such as pdtc once excreted to the environment can perform functions analogous to intracellular thiols. Unlike many other reductive detoxification mechanisms, pdtc-mediated selenite and tellurite reduction can take place in aerobic conditions. The great versatility of pdtc interactions with environmental contaminants, including metalloids, metals, and chlorinated solvents such as carbon tetrachloride, make *P. stutzeri* KC an excellent candidate for use in bioremediation (8, 11). Microbially mediated or biomimetic processes are gaining more interest for remediation technology since they often present solutions that are more cost-effective and of lower environmental impact. Microbial metabolism can substantially influence metal speciation and thus metal mobility and toxicity. Therefore, microbially driven redox reactions and metal solubilization and precipitation processes such as those involving pdtc need to be investigated in efforts to develop new bioremediation technologies (7, 10, 12, 27, 29, 33, 46). Finally, the physical properties of pdtc-precipitated elemental selenium nanoparticles merit further investigation. They may potentially possess unique properties that could find practical application in the field of nanotechnology (31).

ACKNOWLEDGMENTS

This research was supported by an Inland Northwest Research Alliance Subsurface Science Research Institute Ph.D. fellowship to A. Zawadzka (no. 60-4006-102) and by the Environmental Biotechnology Institute at the University of Idaho. We acknowledge the M. J. Murdock Charitable Trust for providing funding to the University of Idaho for EDS and MS equipment and the Idaho BRIN/INBRE program for supporting instrumentation needs in the Environmental Biotechnology Institute's Molecular Ecology and Genomics Laboratory.

We thank Chris Davitt and Franklin Bailey from the Electron Microscopy Centers at Washington State University and at the University of Idaho, respectively. We also thank Janice Strap and two anonymous reviewers for technical review of the manuscript and Cornelia Sawatzky for editorial help.

REFERENCES

1. **Avazéri, C., R. J. Turner, J. Pommier, J. H. Weiner, G. Giordano, and A. Verméglio.** 1997. Tellurite reductase activity of nitrate reductase is responsible for the basal resistance of *Escherichia coli* to tellurite. Microbiology **143:**1181–1189.
2. **Bagnall, K. W.** 1975. Selenium, tellurium, and polonium, p. 935–1008. *In* M. Schmidt, W. Siebert, and K. W. Bagnall (ed.), The chemistry of sulfur, selenium, tellurium, and polonium. Pergamon Press, New York, N.Y.
3. **Basnayake, R. S., J. H. Bius, O. M. Akpolat, and T. G. Chasteen.** 2001. Production of dimethyl telluride and elemental tellurium by bacteria amended with tellurite or tellurate. Appl. Organometal. Chem. **15:**499–510.
4. **Bébien, M., J. Kirsch, V. Méjean, and A. Verméglio.** 2002. Involvment of a putative molybdenum enzyme in the reduction of selenate by *Escherichia coli*. Microbiology **148:**3865–3872.
5. **Budzikiewicz, H.** 2003. Heteroaromatic monothiocarboxylic acids from *Pseudomonas* spp. Biodegradation **14:**65–72.
6. **Bultreys, A., and I. Gheysen.** 2000. Production and comparison of peptide siderophores from strains of distantly related pathovars of *Pseudomonas syringae* and *Pseudomonas viridiflava* LMG 2352. Appl. Environ. Microbiol. **66:**325–331.
7. **Chasteen, T. G., and R. Bentley.** 2003. Biomethylation of selenium and tellurium: microorganisms and plants. Chem. Rev. **103:**1–25.
8. **Cortese, M. S., A. J. Paszczynski, T. A. Lewis, J. L. Sebat, V. Borek, and R. L. Crawford.** 2002. Metal chelating properties of pyridine-2,6-bis(thiocarboxylic acid) produced by *Pseudomonas* spp. and the biological activities of the formed complexes. Biometals **15:**103–120.
9. **Criddle, C. S., J. T. DeWitt, D. Grbic-Galic, and P. L. McCarty.** 1990. Transformation of carbon tetrachloride by *Pseudomonas* sp. strain KC under denitrification conditions. Appl. Environ. Microbiol. **56:**3240–3246.
10. **Diels, L., N. van der Lelie, and L. Bastiaens.** 2002. New developments in treatment of heavy metal contaminated soils. Rev. Environ. Sci. Biotechnol. **1:**75–82.
11. **Dybas, M. J., M. Barclona, S. Bezborodnikov, S. Davies, L. Forney, H. Heuer, O. Kawka, T. Mayotte, L. D. C. Sepulveda-Torres, C. Smalla, M. Sneathen, J. Tiedje, T. Voice, D. D. Wiggert, M. E. Witt, and C. S. Criddle.** 1998. Pilot-scale evaluation of bioaugmentation for in-situ remediation of a carbon tetrachloride-contaminated aquifer. Environ. Sci. Technol. **32:**3598–3611.
12. **Gadd, G. M.** 2004. Microbial influence on metal mobility and application for bioremediation. Geoderma **122:**109–119.
13. **Ganther, H. E.** 1971. Reduction of the selenotrisulfide derivative of glutathione to a persulfide analog by glutathione reductase. Biochemistry **10:**4089–4098.
14. **Gerrard, T. L., J. R. Telford, and H. H. Williams.** 1974. Detection of selenium deposits in *Escherichia coli*. J. Bacteriol. **119:**1057–1060.
15. **Hildebrand, U., W. Ockels, J. Lex, and H. Budzikiewicz.** 1983. Zur struktur eines 1:1-adduktes von pyridin-2,6-dicarbothiosäure und pyridin. Phosphorus Sulfur **16:**361–364.
16. **Hockin, S. L., and G. M. Gadd.** 2003. Linked redox precipitation of sulfur and selenium under anaerobic conditions by sulfate-reducing bacterial biofilms. Appl. Environ. Microbiol. **69:**7063–7072.
17. **Hu, X. C., and G. L. Boyer.** 1996. Siderophore-mediated aluminum uptake by *Bacillus megaterium* ATCC 19213. Appl. Environ. Microbiol. **62:**4044–4048.
18. **Kessi, J., and K. W. Hanselmann.** 2004. Similarities between the abiotic reduction of selenite with glutathione and the dissimilatory reaction mediated by *Rhodospirillum rubrum* and *Escherichia coli*. J. Biol. Chem. **279:**50662–50669.
19. **Kessi, J., M. Ramuz, E. Wehrli, M. Spycher, and R. Bachofen.** 1999. Reduction of selenite and detoxification of elemental selenium by the phototropic bacterium *Rhodospirillum rubrum*. Appl. Environ. Microbiol. **65:**4734–4740.
20. **Klonowska, A., T. Heulin, and A. Vermeglio.** 2005. Selenite and tellurite reduction by *Shewanella oneidensis*. Appl. Environ. Microbiol. **71:**5607–5609.
21. **Lee, C.-H., T. A. Lewis, A. J. Paszczynski, and R. L. Crawford.** 1999. Identification of an extracellular catalyst of carbon tetrachloride dehalogenation from *Pseudomonas stutzeri* strain KC as pyridine-2,6-bis(thiocarboxylate). Biochem. Biophys. Res. Commun. **261:**562–566.
22. **Lee, J. D.** 1996. General properties of the elements, p. 146–193. Concise inorganic chemistry. Blackwell Science, Ltd., Oxford, United Kingdom.
23. **Lee, J. D.** 1996. Group 16: the chalcogens, p. 532–581. Concise inorganic chemistry. Blackwell Science, Ltd., Oxford, United Kingdom.
24. **Lewis, T. A., M. S. Cortese, J. L. Sebat, T. L. Green, C.-H. Lee, and R. L. Crawford.** 2000. A *Pseudomonas stutzeri* gene cluster encoding biosynthesis of the CCl_4-dechlorination agent pyridine-2,6-bis(thiocarboxylic acid). Environ. Microbiol. **2:**407–416.
25. **Lewis, T. A., L. Leach, S. Morales, P. R. Austin, H. J. Hartwell, B. Kaplan, C. Forker, and J. M. Meyer.** 2004. Physiological and molecular genetic evaluation of the dechlorination agent, pyridine-2,6-bis(monothiocarboxylic acid) (PDTC) as a secondary siderophore of *Pseudomonas*. Environ. Microbiol. **6:**159–169.
26. **Lewis, T. A., A. J. Paszczynski, S. W. Gordon-Wylie, S. Jeedigunta, C.-H. Lee, and R. L. Crawford.** 2001. Carbon tetrachloride dechlorination by the bacterial transition metal chelator pyridine-2,6-bis(thiocarboxylic acid). Environ. Sci. Technol. **35:**552–559.
27. **Lloyd, J. R.** 2003. Microbial reduction of metals and radionuclides. FEMS Microbiol. Rev. **27:**411–425.
28. **Lohmeier-Vogel, E. M., S. Ung, and R. J. Turner.** 2004. In vivo ^{31}P nuclear magnetic resonance investigation of tellurite toxicity in *Escherichia coli*. Appl. Environ. Microbiol. **70:**7342–7347.
29. **Nies, D. H.** 1999. Microbial heavy-metal resistance. Appl. Microbiol. Biotechnol. **51:**730–750.
30. **Ockels, W., A. Römer, and H. Budzikiewicz.** 1978. An Fe(III) complex of pyridine-2,6-di(monothiocarboxylic acid): a novel bacterial metabolic product. Tetrahedron Lett. **36:**3341–3342.
31. **Oremland, R. S., M. J. Herbel, J. S. Blum, S. Langley, T. J. Beveridge, P. M. Ajayan, T. Sutto, A. V. Ellis, and S. Curran.** 2004. Structural and spectral features of selenium nanospheres produced by Se-respiring bacteria. Appl. Environ. Microbiol. **70:**52–60.
32. **Painter, E. P.** 1941. The chemistry and toxicity of selenium compounds with special reference to the selenium problem. Chem. Rev. **28:**179–213.
33. **Raab, A., and J. Feldmann.** 2003. Microbial transformation of metals and metalloids. Sci. Prog. **86:**179–202.
34. **Rathgeber, C., N. Yurkova, E. Stackebrandt, J. T. Beatty, and V. Yurkov.** 2002. Isolation of tellurite- and selenite-resistant bacteria from hydrothermal

vents of the Juan de Fuca Ridge in the Pacific Ocean. Appl. Environ. Microbiol. **68:**4613–4622.
35. **Sabaty, M., C. Avazéri, D. Pignol, and A. Verméglio.** 2001. Characterization of the reduction of selenate and tellurite by nitrate reductases. Appl. Environ. Microbiol. **67:**5122–5126.
36. **Schröder, I., S. Rech, T. Krafft, and J. M. Macy.** 1997. Purification and characterization of the selenate reductase from *Thauera selenatis*. J. Biol. Chem. **272:**23765–23768.
37. **Sebat, J. L., A. J. Paszczynski, M. S. Cortese, and R. L. Crawford.** 2001. Antimicrobial properties of pyridine-2,6-dithiocarboxylic acid, a metal chelator produced by *Pseudomonas* spp. Appl. Environ. Microbiol. **67:**3934–3942.
38. **Silver, S.** 1996. Bacterial resistances to toxic metal ions: a review. Gene **179:**9–19.
39. **Stolworthy, J. C., A. J. Paszczynski, R. Korus, and R. L. Crawford.** 2001. Metal binding by pyridine-2,6-bis(monothiocarboxylic acid), a biochelator produced by *Pseudomonas stutzeri* and *Pseudomonas putida*. Biodegradation **12:**411–418.
40. **Sullivan, J. B., F. B. Chen, and R. E. Hodson.** 1999. Constitutive production of nitrite reductase in *Pseudomonas stutzeri* detected by in situ RT-PCR. Code: SS41TU0919S. Aquatic Sciences Meeting, Santa Fe, N.Mex.
41. **Taylor, D. E.** 1999. Bacterial tellurite resistance. Trends Microbiol. **7:**111–115.
42. **Trutko, S. M., V. K. Akimenko, N. E. Suzina, L. A. Anisimova, M. G. Shlyapnikov, B. P. Baskunov, V. I. Duda, and A. M. Boronin.** 2000. Involvement of the respiratory chain of gram-negative bacteria in the reduction of tellurite. Arch. Microbiol. **173:**178–186.
43. **Turner, R. J., Y. Aharonowitz, J. H. Weiner, and D. E. Taylor.** 2001. Glutathione is a target in tellurite toxicity and is protected by tellurite resistance determinants in *Escherichia coli*. Can. J. Microbiol. **47:**33–40.
44. **Turner, R. J., J. H. Weiner, and D. E. Taylor.** 1998. Selenium metabolism in *Escherichia coli*. Biometals **11:**223–227.
45. **Turner, R. J., J. H. Weiner, and D. E. Taylor.** 1999. Tellurite-mediated thiol oxidation in *Escherichia coli*. Microbiology **145:**2549–2557.
46. **Valls, M., and V. de Lorenzo.** 2002. Exploiting the genetic and biochemical capacities of bacteria for the remediation of heavy metal pollution. FEMS Microbiol. Rev. **26:**327–338.
47. **Visca, P., G. Colotti, L. Serino, D. Verzili, N. Orsi, and E. Chiancone.** 1992. Metal regulation of siderophore synthesis in *Pseudomonas aeruginosa* and functional effects of siderophore-metal complexes. Appl. Environ. Microbiol. **58:**2886–2893.
48. **Yamada, A., M. Miyashita, K. Inoue, and T. Matsunaga.** 1997. Extracellular reduction of selenite by a novel marine photosynthetic bacterium. Appl. Microbiol. Biotechnol. **48:**367–372.